Supplementary Information (SI) for Nanoscale.

Supporting Information

Achieving a balance of rapid Zn^{2+} desolvation and hydrogen evolution reaction inertia on the interface of Zn anode ~~by hydrophilic transition metal oxides~~

Xiaofen Xiao*[a], Deqiang Wang[a], Guangyi Xu[a], Zhuxiang Zhang[a], Jun Li[a,b], Shun Wang[a], Yifei Yuan[a], Chuangang Hu[c] and Huile Jin*[a,b]

1 Key Lab of Advanced Energy Storage and Conversion, Zhejiang Province Key Lab of Leather Engineering, College of Chemistry and Materials Engineering, Wenzhou University, Wenzhou, Zhejiang 325035, China

2 Zhejiang Engineering Research Center for Electrochemical Energy Materials and Devices, Institute of New Materials and Industrial Technologies, Wenzhou University, Wenzhou, Zhejiang 325035, China

3 State Key Laboratory of Organic-Inorganic Composites, College of Chemical Engineering, Beijing University of Chemical Technology, Beijing 100029, China

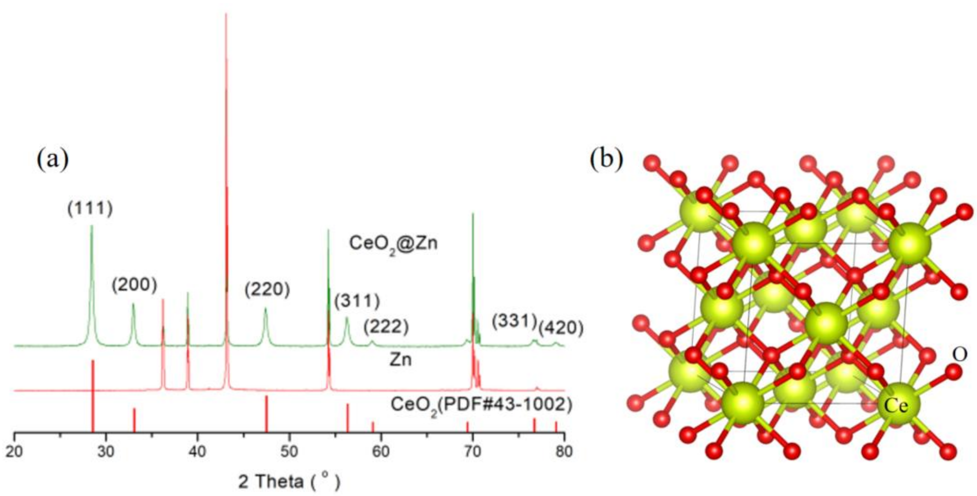

Fig. S1. (a) The XRD patterns of CeO_2 coated Zn foil, (b) crystal structure of CeO_2.

The chemical structure of CeO_2@Zn is also characterized as shown in **Fig. S2**, where the main XRD peaks of the modified Zn anode could be ascribed to the standard CeO_2 (PDF#43-1002), proving that the modified layer of CeO_2 keeps stable in the open air.

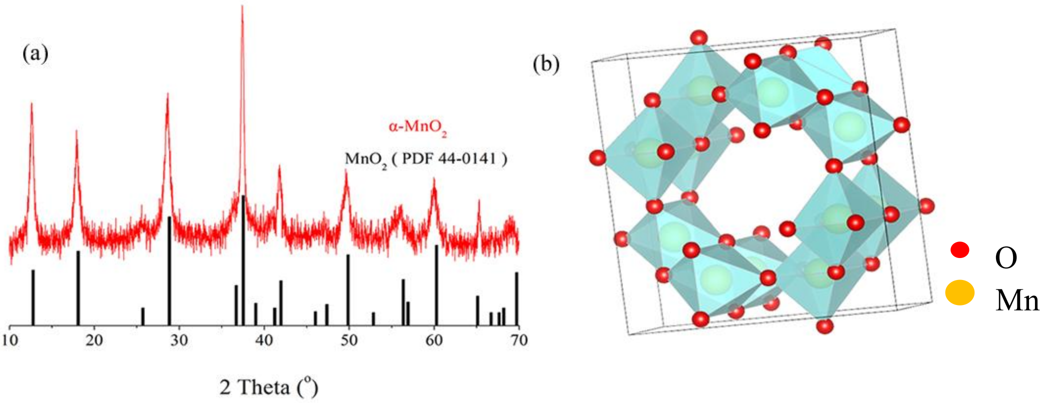

Fig. S2. (a) The XRD patterns of MnO_2 powders and (b) the structure of α-MnO_2 used. It shows the crystalline phase of α-MnO_2 (JCPDS: 44-0141).

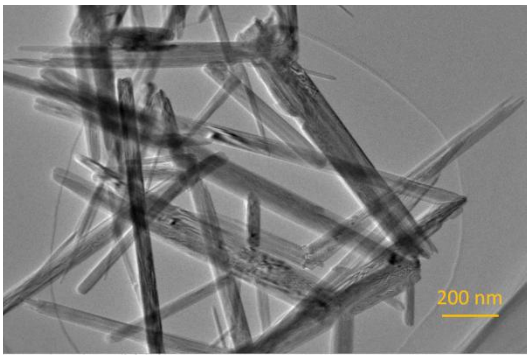

Fig. S3. TEM image of MnO_2 powders used in our experiment. It shows the tunable nanorod morphology of α-MnO_2.

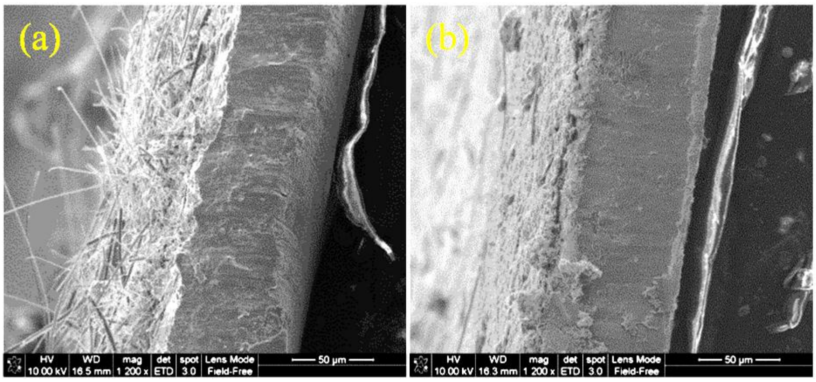

Fig. S4. The cross-section SEM images of the cycled Zn plates: (a) bare Zn and (b) CeO_2@Zn.

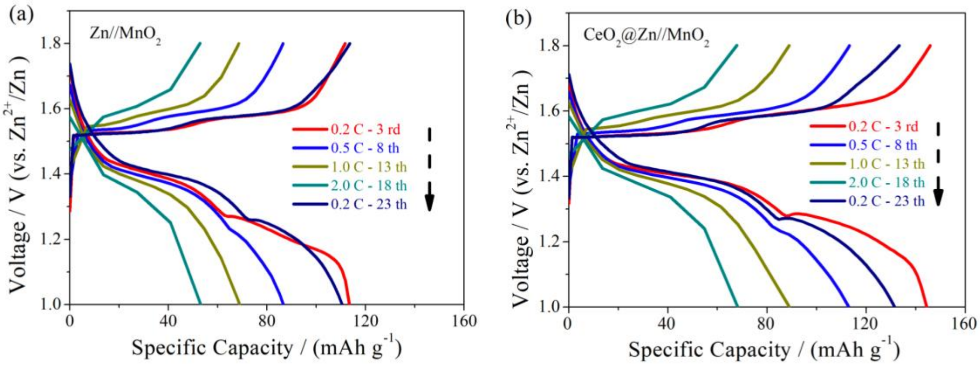

Fig. S5. GCD profiles of the aqueous Zn//MnO_2 and CeO_2@Zn//MnO_2 batteries at C-rate of 0.2-2.0 C corresponding to **Fig. 3-6d**.

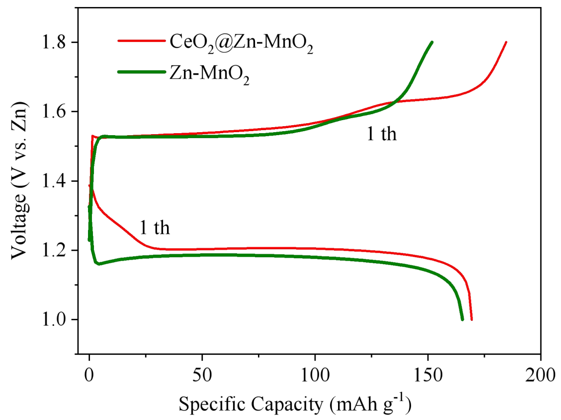

Fig. S6. The first charge/discharge profiles of Zn//MnO_2 and CeO2@MnO_2 under 0.2 C (corresponding to the data in **Fig. 4d**).

It can be seen from **Fig. S6** that the specific capacity was 169.36 mAh g^{-1} and 165.26 mAh g^{-1}, for Zn//MnO_2 and CeO_2@Zn//MnO_2 full cells, respectively.

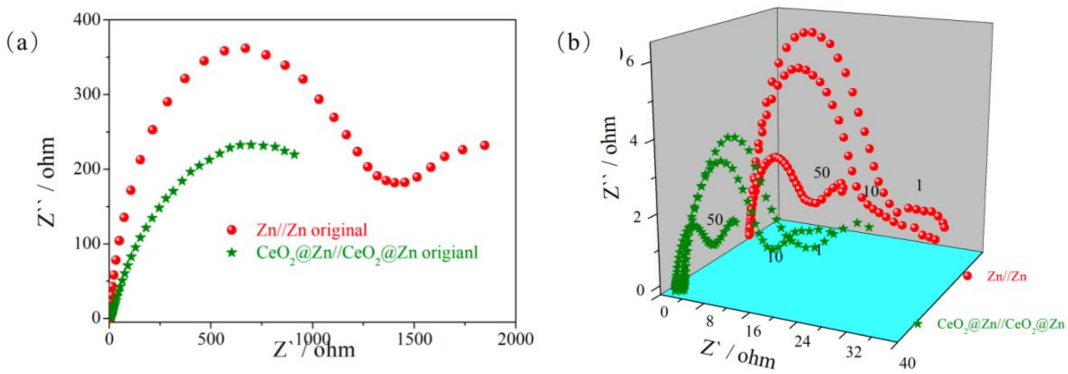

Fig. S7. Nyquist plots of Zn//Zn and CeO_2@Zn//CeO_2@Zn under different cycling numbers.

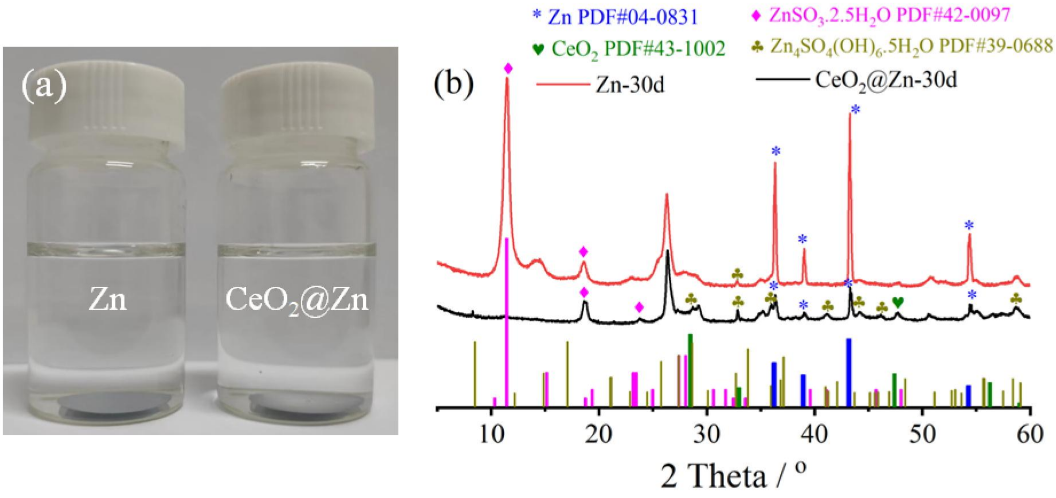

Fig. S8. (a) the digital photo of CeO_2@Zn and Zn immersed in 2 M $ZnSO_4$ for 7 days, (b) the corresponding XRD patterns of (a).

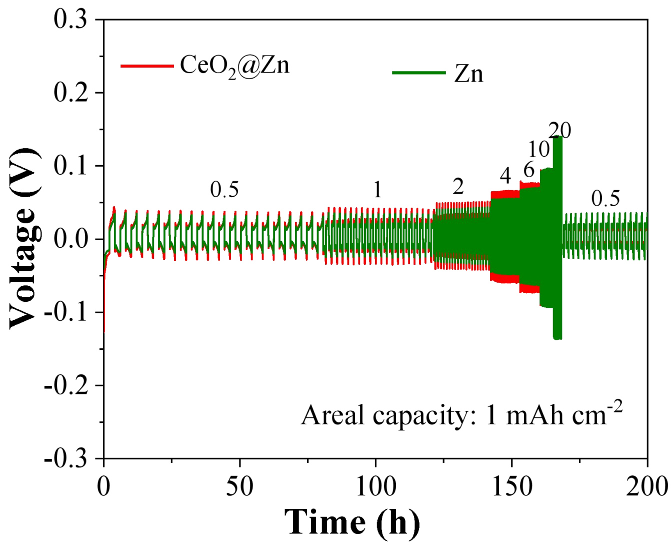

Fig. S9. Rate capability of CeO_2@Zn and Zn symmetry batteries.

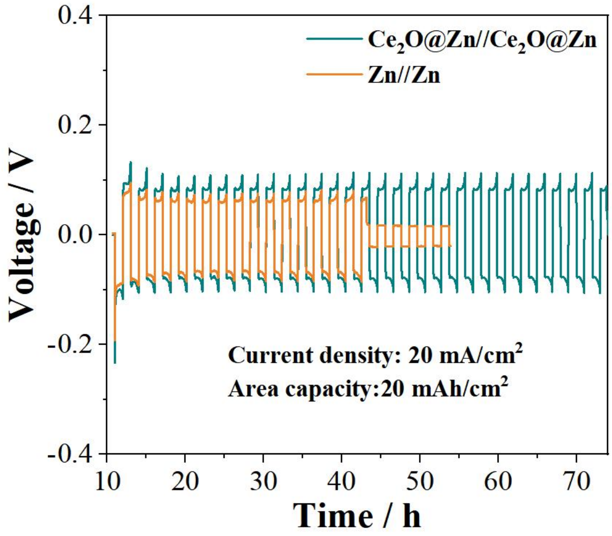

Fig. S10. Voltage profiles of symmetric cells based on Zn foil and CeO_2@Zn anode at 20 mA cm^{-2} with a total capacity of 20 mAh cm^{-2}.

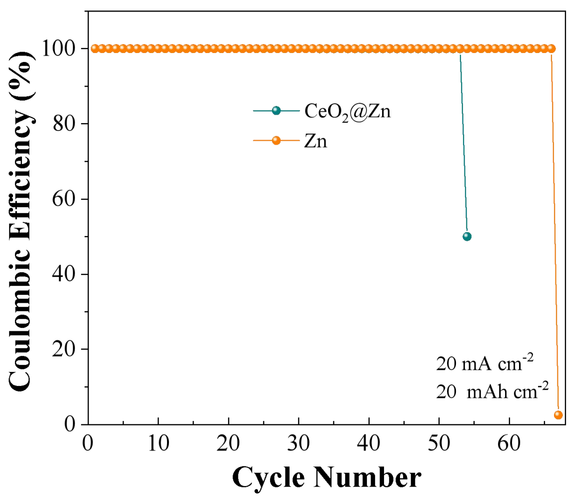

Fig. S11. CE of the symmetric Zn//Zn and CeO_2@Zn//CeO_2@Zn at a current density of 20 mA cm^{-2} with a total capacity of 20 mAh cm^{-2}. (corresponding to **Fig. S10**).

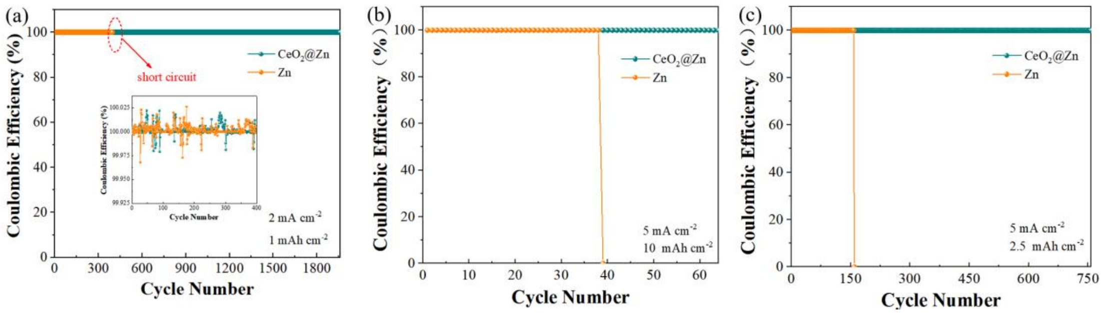

Fig. S12. CE of the symmetric Zn//Zn and CeO_2@Zn//CeO_2@Zn at a current density of (a) 2.0 mA cm^{-2} with a total capacity of 1.0 mAh cm^{-2}, (b) 5 mA cm^{-2} with a total capacity of 10 mAh cm^{-2} and (c) 5 mA cm^{-2} with a total capacity of 2.5 mAh cm^{-2}. (corresponding to **Fig. 2a-c**)

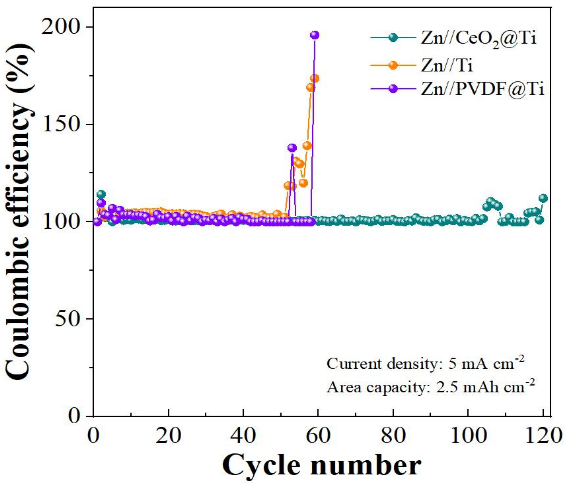

Fig. S13. CE of the asymmetric Zn//Ti, PVDF@Ti and Zn //CeO_2@Ti at 5.0 mA cm^{-2}, 2.5 mAh cm^{-2} with an end charging voltage of 0.5 V (The thickness of the Zn foil here was 30μm).

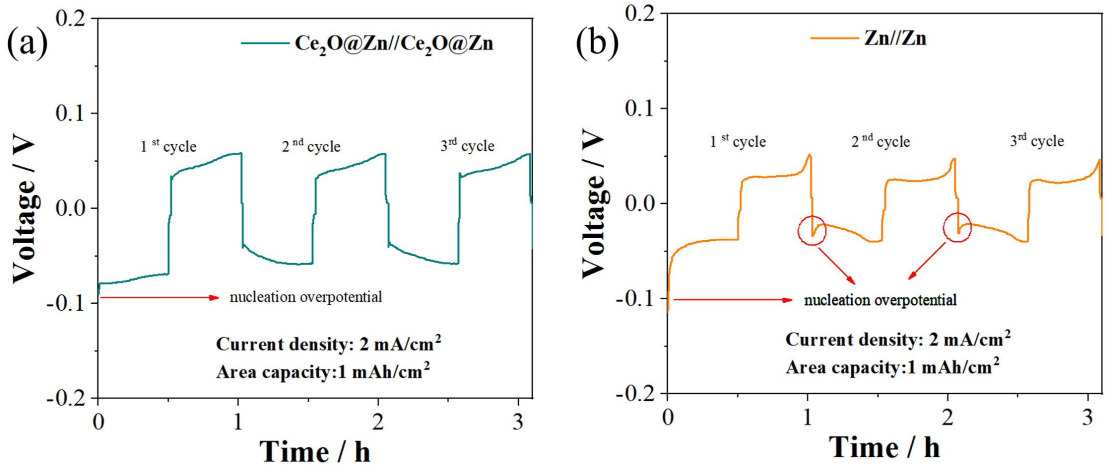

Fig. S14. Overpotential evolution of symmetric Zn//Zn and CeO_2@Zn//CeO_2@Zn cells at a current density of 2.0 mA cm^{-2} with a total capacity of 1.0 mAh cm^{-2}.

In Zn//Zn cell, each Zn^{2+} deposition process has a typical nucleation overpotential. However, there is no obvious nucleation overpotential in the overpotential evolution curve of CeO_2@Zn//CeO_2@Zn cell except the initial nucleation overpotential, which shows that CeO_2 coating layer reduces the energy barrier of Zn^{2+} nucleation and changes the deposition process of Zn^{2+} compared with that of bare Zn.

Table S1. Comparison of electrochemical properties of the reported Zn anode after being optimized in various electrolytes.

Strategies	Cycling performance of symmetrical Zn battery	Volta Hysteresis (mV)	References
CeO_2@Zn	1600 h (2 mA/cm^2, 1 mAh/cm^2)	~ 50	This work
	750 h (5 mA/cm^2, 2.5 mAh/cm^2)	~	
	150 h (5 mA/cm^2, 10 mAh/cm^2)	~ 50	
PVDF-TiO_2-Zn	2000 h (0.885 mA/cm^2, 0.885 mAh/cm^2)	< 50	Adv. Funct. Mater. 2020, 2001867
	250 h (20 mA/cm^2, 10 mAh/cm^2)	~	
Zn	300 h (0.885 mA/cm^2, 0.885 mAh/cm^2)	~ 70	
	< 30 h (20 mA/cm^2, 10 mAh/cm^2)	~	
Electrodopsition CNT-Zn	200 h (2 mA/cm^2, 2 mAh/cm^2)	27	Adv. Mater. 2019, 31, 1903675
	110 h (5 mA/cm^2, 2.5 mAh/cm^2)	68	
Zn foil	43 h (5 mA/cm^2, 2.5 mAh/cm^2)	79	
Electrodopsition CC-Zn	53 h (2 mA/cm^2, 2 mAh/cm^2)	34	
TiO_2@Zn	460 h (1 mA/cm^2, 1 mAh/cm^2)	~	Nat Commun 11, 3961 (2020).
	280 h (2 mA/cm^2, 2 mAh/cm^2)		
nano-$CaCO_3$ @Zn foil	836 h (0.25 mA/cm^2, 0.05 mAh/cm^2)	80	Adv. Energy Mater. 2018, 8, 1801090
nano-SiO2@Zn foil	~ 400 h (0.25 mA/cm^2, 0.05 mAh/cm^2)		
Bare Zn foil	55 h (0.25 mA/cm^2, 0.05 mAh/cm^2)	230	
ZnS @ Zn-350	1100 h (2mA/cm^2, 2 mAh/cm^2)	98	Adv. Mater. 2020, 32, 2003021
Bare Zn	100 h (2mA/cm^2, 2 mAh/cm^2)	150	
ZIF-8@Zn	1200 h (2mA/cm^2, 2 mAh/cm^2)	58	Adv. Sci. 2020, 7, 2002173
ZIF-8-500@Zn	200 cycles (1 mA/cm^2, 2 mAh/cm^2)		Joule 3, 1289–1300, May 15, 2019
polyamide-Zn	8000 h (0.5 mA/cm^2, 0.25 mAh/cm^2)	~100	Energy Environ. Sci., 2019, 12, 1938--1949
	(10 mA/cm^2, 10 mAh/cm^2)		
cyanoacrylate 502 glue-Zn	800 h (0.5 mA/cm^2, 0.25 mAh/cm^2)	~	Energy Storage Materials 36 (2021) 132-138.
	400 h (2 mA/cm^2, 1 mAh/cm^2)	91.3	
$In(OH)_2$@Zn	1500 h (0.2 mA/cm^2, 0.2 mAh/cm^2)	54	Small 2020, 16, 2001736.